VII International Conference on Computational Methods in Marine Engineering
MARINE 2017
M. Visonneau, P. Queutey and D. Le Touzé (Eds)

MONOLITHIC COUPLING OF RIGID BODY MOTION AND THE PRESSURE FIELD IN FOAM-EXTEND

Inno Gatin*, Vuko Vukčević, Hrvoje Jasak

University of Zagreb, Faculty of Mechanical Engineering and Naval Architecture,
Ivana Lučića 5, Zagreb, Croatia
e-mail: inno.gatin@fsb.hr, vuko.vukcevic@fsb.hr, hrvoje.jasak@fsb.hr

Key words: CFD, foam–extend, Rigid Body Motion, Seakeeping

Abstract. In this paper a monolithic algorithm for coupling rigid body motion equations and pressure field within a Finite Volume framework is presented. Monolithic coupling enables fewer number of pressure–velocity loops per time–step, thus reducing the required computational time. The presented method is compared to conventional partitioned coupling approach in terms of computational efficiency and accuracy. The results are compared to experimental data as well.

1 INTRODUCTION

The interaction between a floating rigid body and free surface waves is a problem often encountered in the field of naval hydrodynamics. The complexity of the problem encouraged utilisation of viscous Computational Fluid Dynamics (CFD) codes, where the interaction between the two–phase, viscous flow and the rigid body can be fully resolved. The forces acting on the rigid body are a result of combined pressure and viscous effects which the fluid exerts upon the boundary of the rigid body. The oscillatory nature of forces exerted on the body due to surface waves are dominated by the change in pressure forces, while viscous effects play a minor role in the oscillatory motion. Hence, given the segregated nature of the pressure–velocity coupling in modern CFD algorithms, it is necessary to properly resolve the interaction between the body motion and the pressure field in each time–step.

Conventional approach for resolving rigid body motion and fluid flow coupling solves the body motion equations once per pressure–velocity coupling loop. In transient simulations, multiple pressure–velocity coupling loops are necessary in order to obtain convergence of fluid flow. The introduction of body motion increases the number of necessary pressure–velocity coupling loops per time–step, since it represents a flow–dependent moving boundary. It is the intention to avoid the increase in the number of pressure–velocity coupling loops.

In this work the pressure–body motion coupling is resolved on the linear solver level of the pressure equation. Hence, monolithic coupling between the pressure equation and rigid body motion equations is achieved. The monolithic coupling leads to a fully resolved pressure–body motion coupling at the end of every pressure equation solution. Hence, no additional pressure–velocity loops are needed on the account of the rigid body motion.

The performance of the novel approach is compared to the conventional partitioned approach on a seakeeping benchmark case of a KCS hull from Tokyo 2015 Ship Hydrodynamics workshop [1]. The comparison shows that similar accuracy in terms of motion and added resistance is obtained while using a smaller number of pressure–velocity correctors per time–step. The results are compared to experimental values in order to validate the method.

Naval Hydro software pack based on foam-extend is used which is specialised for simulating large scale, two–phase flows in Finite Volume (FV) framework. Regular waves are imposed using SWENSE (Spectral Wave Explicit Navier Stokes Equations) method [2, 3], which allows accurate and robust two–phase simulations. Implicitly redistanced Level Set method is used for interface capturing, while Ghost Fluid Method [4] is employed to discretise the dynamic free surface boundary condition, enhancing the stability of the simulation.

The paper is organised as follows. First, the mathematical formulation of the monolithic pressure–body motion coupling is presented. Second, the comparison of the developed method against a conventional partitioned coupling scheme is shown, followed by a comparison with the experimental results. Finally, a conclusion is given.

2 MATHEMATICAL MODEL

Governing equations for two–phase, viscous, incompressible flow are given by the conservation of linear momentum and mass:

$$\frac{\partial \mathbf{u}}{\partial t} + \nabla \bullet ((\mathbf{u} - \mathbf{u}_M)\, \mathbf{u}) - \nabla \bullet (\nu_e \nabla \mathbf{u}) = -\frac{1}{\rho} \nabla p_d \,, \tag{1}$$

$$\nabla \bullet \mathbf{u} = 0 \,, \tag{2}$$

where $\mathbf{u}$ presents the velocity field, $\mathbf{u}_M$ is the velocity of the relative grid motion [5], ν_e is the effective kinematic viscosity, while ρ is the respective phase density. p_d is the dynamic pressure calculated as $p_d = p - \rho \mathbf{g} \bullet \mathbf{x}$, where p denotes the total pressure, $\mathbf{g}$ is the gravity constant and $\mathbf{x}$ is the radii vector.

The rigid body motion can be taken into account in the continuity equation, Eq. (2), by accounting for the change of body boundary velocity $\delta \mathbf{u}_b$:

$$\nabla \bullet \mathbf{u} + \nabla \bullet (\delta \mathbf{u}_b) = 0 \,. \tag{3}$$

By discretising Eq. (1) and Eq. (3) in the FV method fashion [6], Eq. (3) becomes:

$$\sum_f \mathbf{s}_f \bullet \left(\frac{1}{a_P} \right)_f \left(\frac{\nabla p_d}{\rho} \right)_f = \sum_f \mathbf{s}_f \bullet \frac{(\mathbf{H}(\mathbf{u}_N))_f}{(a_P)_f} - \sum_f \mathbf{s}_f \bullet \delta \mathbf{u}_{bf} \,, \tag{4}$$

where f presents the cell face index, $\mathbf{s}_f$ is the face surface normal vector with a magnitude corresponding to the area of the face, a_P is the diagonal contribution of the discretised momentum equation, Eq.(1), while $\mathbf{H}(\mathbf{u}_N)$ presents a linear function of the neighbouring cell velocities $\mathbf{u}_N$ which stems from the off–diagonal and source contribution of the discretised momentum equation. Eq. (4) is a conventional pressure eqution, with an additional term on the right hand side which accounts for the change in the body boundary velocity. This way the pressure is coupled to the rigid body motion on the equation level.

In order to obtain the change of boundary velocity $\delta \mathbf{u}_b$ the rigid body motion equations need to be integrated:

$$\frac{\partial \mathbf{v}}{\partial t} = \frac{\mathbf{F}}{m}\,, \qquad (5)$$
$$\frac{\partial \boldsymbol{\omega}}{\partial t} = \mathbf{I}^{-1} \bullet (\mathbf{M} - \boldsymbol{\omega} \times (\mathbf{I} \bullet \boldsymbol{\omega}))\,,$$

where $\mathbf{v}$ denotes the translational velocity of the centre of mass, $\mathbf{F}$ is the external force exerted on the body and m stands for the mass of the body. $\boldsymbol{\omega}$ is the angular velocity vector, $\mathbf{I}$ is the inertia tensor of the rigid body, while $\mathbf{M}$ denotes the external moment. The external force and moment are calculated by integrating the pressure and viscous stress on the body boundary:

$$\mathbf{F} = \sum_{bf} \mathbf{s}_{bf} p_{bf} + \mathbf{F}_v\,, \qquad (6)$$
$$\mathbf{M} = \sum_{bf} \mathbf{r}_{bf} \times \mathbf{s}_{bf} p_{bf} + \mathbf{M}_v\,,$$

where bf stands for the body boundary face index, $\mathbf{s}_{bf}$ is the normal surface vector of the boundary face with the magnitude corresponding to the surface area of the face, p_{bf} is the total pressure acting on the boundary face. $\mathbf{r}_{bf}$ is the radii vector of the face centre with respect to the centre of gravity. $\mathbf{F}_v$ and $\mathbf{M}_v$ denote the viscous portion of the force and moment acting on the rigid body boundary, respectively, which are treated explicitly.

Finally, the change of the boundary face velocity $\delta \mathbf{u}_{bf}$ is obtained as the difference of the translational and rotational velocity:

$$\delta \mathbf{u}_{bf}^n = \mathbf{v}^n - \mathbf{v}^{n-1} + \left(\boldsymbol{\omega}^n - \boldsymbol{\omega}^{n-1}\right) \times \mathbf{x}_{bf}\,, \qquad (7)$$

where n denotes the linear solver iteration. Hence the equation set forming the pressure–rigid body motion coupling, which comprises Eq. (4) and Eq. (5) is closed by relations expressed with Eq. (6) and Eq. (7). These relations are evaluated at the level of pressure equation linear solver, Eq. (4), where the updated pressure solution is used to reintegrate the rigid body motion equations, Eq. (5).

3 NUMERICAL METHODS

In this work the Naval Hydro software pack is used, which is based on foam–extend CFD open–source software. Naval Hydro provides specialised numerical solvers for simulating large–scale, two–phase, viscous and turbulent flows. Ghost Fluid Method is used to discretise the dynamic and kinematic free surface boundary conditions [4], which eliminates the parasitic air currents present in many two–phase CFD codes. SWENSE method [2, 3] is employed to impose an arbitrary wave solution into the CFD model, where only the difference between the imposed flow solution and the full nonlinear solution is solved for. SWENSE enhances the accuracy of wave propagation in CFD and enables coarser temporal and spatial resolution while minimising the diffusion and dispersion of the wave field propagating through the CFD domain.

In this work a preconditioned Conjugate Gradient [7] method is used for solving the linear system arising from the discretised pressure equation. Fifth-order Cash-Karp embedded Runge–Kutta scheme with error control and adjustive time-step size [8] is used for rigid body motion integration.

4 SEAKEEPING

In this section, a regular head wave seakeeping case is considered. The wave and ship velocity setup correspond to case C5 from the Tokyo Workshop on CFD in Ship Hydrodynamics [9], where the model scale KCS hull is used. In order to investigate the possible benefits of the new method, the two coupling strategies for pressure–rigid body motion coupling are compared, where the number of pressure–velocity loops per time–step is varied. Simulations using 2, 4 and 8 pressure–velocity loops are carried out, with four pressure correctors used per one pressure–velocity loop in all simulations.

The same computational mesh is used in all simulations, where half of the domain is simulated due to the symmetry of the phenomenon. Extremely coarse spatial discretisation is used, counting only 600 000 cells. Temporal resolution is set to 400 time steps per encounter wave period. The ship is free to pitch and heave, while a fixed surge velocity is prescribed. Nine items are compared in total: mean, first order amplitudes and first order phases of total resistance coefficient C_T, heave z and pitch ϕ.

The comparison is shown in Fig. 1, where all nine items are compared with respect to the number of pressure–velocity loops per time step. The first row of graphs show the comparison for the total resistance coefficient C_T. The second row shows dimensionless heave, while the third row shows dimensionless pitch. η denotes the regular wave amplitude and k stands for the wave number. The mean of an item is indicated with the subscript 0, and the first order amplitude with subscript 1. The first order phases are denoted with γ, where the subscript denotes the item the phase corresponds to. For most items, the monolithic approach exhibits low sensitivity with respect to the number of pressure–velocity loops. Moreover, with two pressure–velocity loops per time–step the monolithic approach produces similar results to the partitioned approach with eight pressure–velocity loops. This is true for all items related to resistance, first order amplitude of heave and pitch and for the first order phase of heave. Hence, the monolithic coupling enables accurate estimation of the most important seakeeping items, i.e. mean of total resistance and first order amplitudes of motion, with four times smaller number of pressure–velocity loops per time–step. For mean of pitch and heave, and for the first order phase of pitch, the two coupling strategies exhibit similar convergence patterns. It should be noted that mean of pitch ϕ_0 has very small absolute values which cannot be captured with the coarse spatial discretisation that was used in the simulations.

Fig. 2 shows the required computational time per time–step for the monolithic and partitioned approach with respect to the number of pressure–velocity loops per time–step. The monolithic approach requires more computational time for the same number of pressure–velocity loops due to the additional integrations of the rigid body motion equation. However, since only two instead of eight pressure–velocity loops can be used with the monolithic approach, a total saving in computational time of a factor by 2.4 is achieved.

In order to validate the method, the results of both methods obtained with eight pressure–velocity loops are compared to the experiment. Table 1 shows the relative errors of all items for two coupling strategies. The relative error is computed as $E = (EFD - CFD)/EFD$, where CFD represents the result obtained using the computational method, while EFD stands for experimental result. The subscript denotes the item to which the relative error corresponds to. Given the extremely low spatial resolution used in these simulations, relative errors are satisfac-

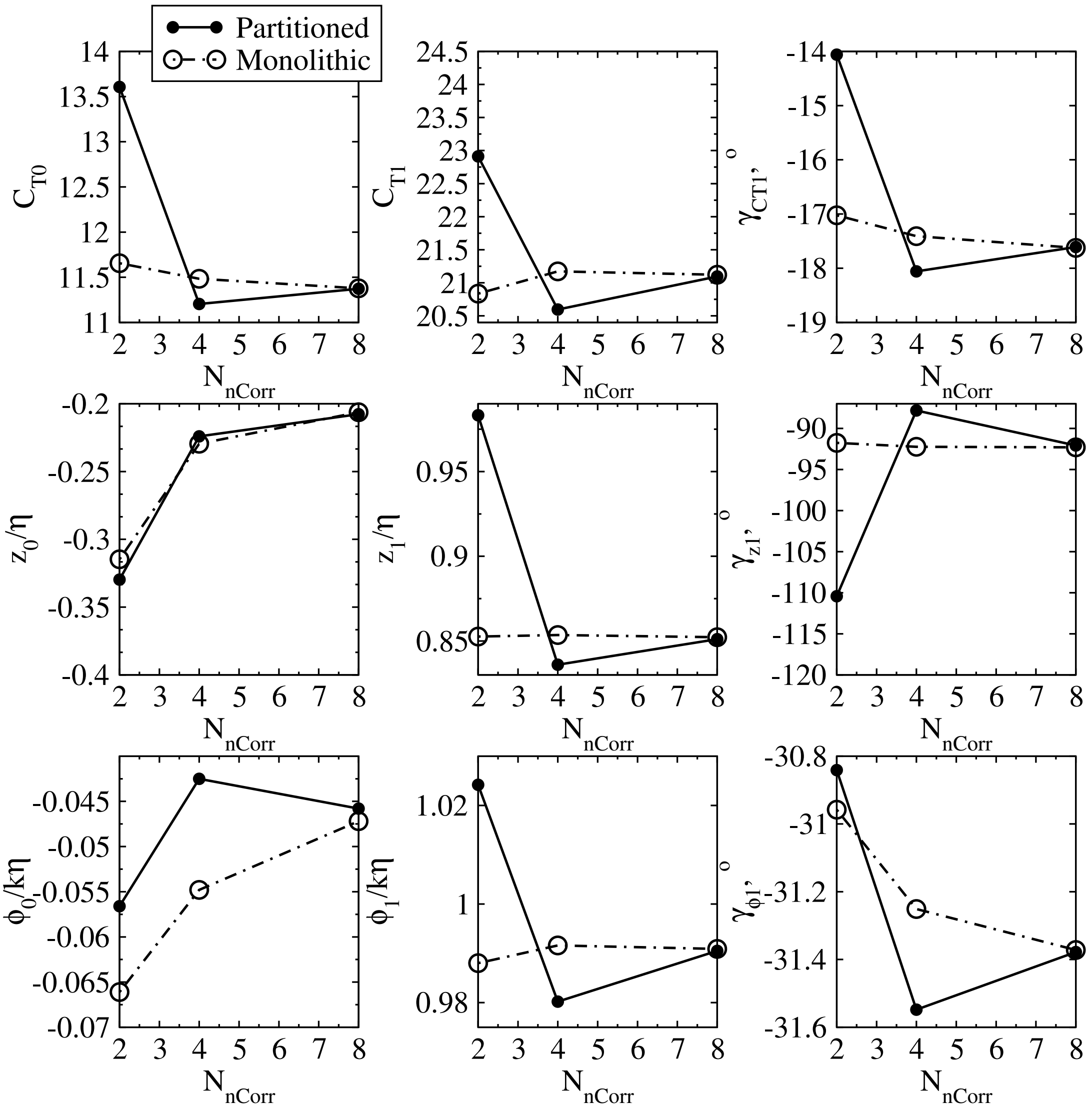

Figure 1: **Comparison of seakeeping results of partitioned and monolithic approach for pressure–rigid body motion coupling, with respect to the number of pressure–velocity loops per time–step** N_{nCorr}.

tory. The monolithic and partitioned approach have similar errors, which validates the present approach, since the partitioned approach has been thoroughly validated and verified in previous publications [10, 11].

5 CONCLUSION

Monolithic pressure–rigid body motion coupling method in FV numerical framework is presented in this paper. The new approach is intended for pressure dominated fluid–rigid body interaction problems, which are often encountered in the field of computational naval hydro-

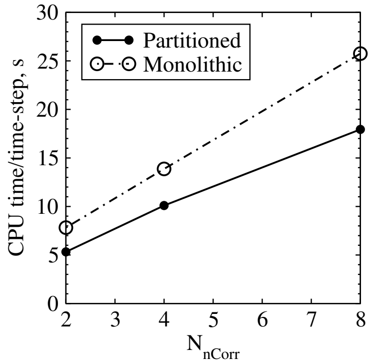

Figure 2: **Comparison of required computational time per time–step with respect to the number of pressure–velocity loops per time–step N_{nCorr}.**

Table 1: Result comparison with experimental data.

	Monolithic	Partitioned
$E_{C_{T0}}$, %	-4.95	-4.90
$E_{C_{T1}}$, %	15.85	15.96
$E_{\gamma_{CT1}}$, %	14.20	14.29
E_{z_0}, %	-2.86	-3.60
E_{z_1}, %	8.48	8.60
$E_{\gamma_{z1}}$, %	6.37	6.59
E_{ϕ_0}, %	16.09	18.50
E_{ϕ_1}, %	11.41	11.44
$E_{\gamma_{\phi1}}$, %	5.77	5.76

dynamics. The method is tested on a seakeeping case and compared in terms of accuracy and performance against the conventional partitioned approach. Results are compared to experimental data to validate the approach.

The comparison of the monolithic and partitioned approach shows that monolithic approach requires fewer pressure–velocity loops per time–step for the pressure–rigid body motion coupling to be properly resolved. Only two pressure–velocity loops are sufficient to obtain similar accuracy to the partitioned approach where eight pressure–velocity loops are employed. The reduction in the number of pressure–velocity loops per time–step reduces the computational time by a factor of 2.4. Comparison with experimental data validates the monolithic approach, where similar accuracy is achieved to the partitioned approach.

The monolithic pressure–rigid body motion coupling presents an advance coupling algorithm, which enables considerable acceleration in computational time. It is applicable to many problems in the field of naval hydrodynamics where the naval object can be considered as rigid.

REFERENCES

[1] National Maritime Reasearch Inistitute (NMRI), Tokyo 2015: A Workshop on CFD in Ship Hydrodynamics, `http://www.t2015.nmri.go.jp/`, [Online; accessed 20 August 2015] (2015).

[2] V. Vukčević, H. Jasak, S. Malenica, Decomposition model for naval hydrodynamic applications, Part I: Computational method, Ocean Eng. 121 (2016) 37–46. doi:10.1016/j.oceaneng.2016.05.022.

[3] V. Vukčević, H. Jasak, S. Malenica, Decomposition model for naval hydrodynamic applications, Part II: Verification and validation, Ocean Eng. 121 (2016) 76–88. doi:10.1016/j.oceaneng.2016.05.021.

[4] V. Vukčević, Numerical modelling of coupled potential and viscous flow for marine applications, Ph.D. thesis, Faculty of Mechanical Engineering and Naval Architecture, University of Zagreb, PhD Thesis (2016).

[5] I. Demirdžić, M. Perić, Space conservation law in finite volume calculations of fluid flow, International journal for numerical methods in fluids 8 (9) (1988) 1037–1050.

[6] H. Jasak, Error analysis and estimation for the finite volume method with applications to fluid flows, Ph.D. thesis, Imperial College of Science, Technology & Medicine, London (1996).

[7] Y. Saad, Iterative Methods for Sparse Linear Systems (2nd Edition), Society for Industrial and Applied Mathematics Philadelphia, SIAM, 2003.

[8] W. H. Press, S. A. Teukolsky, W. T. Vetterling, B. P. Flannery, Numerical Recipes in C++: The Art of Scientific Computing, Cambridge University Press, 2002.

[9] L. Larsson, F. Stern, M. Visonneau, N. Hirata, T. Hino, J. Kim (Eds.), Tokyo 2015: A Workshop on CFD in Ship Hydrodynamics, Vol. 3, NMRI (National Maritime Research Institute), Tokyo, Japan, 2015.

[10] V. Vukčević, H. Jasak, Seakeeping validation and verification using decomposition model based on embedded free surface method, in: Tokyo 2015: A workshop on CFD in Ship Hydrodynamics, 2015.

[11] V. Vukčević, H. Jasak, Validation and Verification of Decomposition Model based on Embedded Free Surface Method for Oblique Wave Seakeeping Simulations, in: Tokyo 2015: A workshop on CFD in Ship Hydrodynamics, 2015.